13th International Conference on Fracture
June 16–21, 2013, Beijing, China

Elastodynamic analysis of a finite crack at an arbitrary angle in the functionally graded material under in-plane impact loading

Sheng-Hu Ding*, Xing Li
School of Mathematics and Computer Science, Ningxia University, Yinchuan, 750021, China
*Corresponding author:Email:dshsjtu2009@163.com

Abstract The plane problem for a infinite functionally graded material containing a finite crack subjected to the dynamic impact loads is investigated. The crack arbitrarily oriented with respect to the direction of property gradient is considered. Based on the use of Laplace and Fourier integral transforms, formulation of the transient crack problem is reduced to solving a system of Cauchy-type singular integral equation in the Laplace transform domain. The crack-tip response in the physical domain is recovered via the inverse Laplace transform and the values of dynamic stress intensity factors are obtained as a function of time. The effects come from the crack orientation and the nonhomogeneous material parameter on the dynamic stress intensity factors are discussed graphically.

Keywords Functionally graded material, Arbitrarily oriented crack, Singular integral equations, Dynamic stress intensity factors

1. Introduction

With the application of functionally gradient materials in engineering, most of the current researches [1-5] on the fracture analysis of the FGMs interface have been devoted to the FGMs interlayer and the interface between the functionally graded material (FGM) coating and the homogeneous substrate. However, to date, only a few articles were devoted to the dynamic fracture mechanics of FGMs. Among these limited work, Atkinson [6] first studied the crack propagation in media with spatially varying elastic properties. Li and Wen [7] investigated the dynamic stress intensity factor of a cylindrical interface crack located between two coaxial dissimilar homogeneous cylinders that are bonded with a functionally graded interlayer and subjected to a torsional impact loading. The transient response of a functionally graded coating-substrate system with an internal or edge crack perpendicular to the interface [8] has been studied under an in-plane impact load. Recently, the dynamic fracture problem of the weak-discontinuous interface between a FGM coating and a FGM substrate have been studied by Li and his coauthors [9]. Ding and Li [10] studied the dynamic stress intensity factor of collinear crack-tip fields in bonded functionally graded finite strips.

For the arbitrarily oriented crack, Bogy [11] studied the problem of an arbitrarily oriented crack terminated at the bonded interface. For FGMs, till 1994 when Konda and Erdogan [12] considered the mixed mode crack problem in a nonhomogeneous elastic medium. Under the condition of antiplane shear impact, the corresponding dynamic stress intensity factors for a crack in a homogeneous material when a graded stip between dissimilar half-planes was evaluated by Choi [13].

The objective of the present paper is to provide a theoretical analysis of the dynamic behavior of a finite crack in the functionally graded material subjected to in-plane impact loading. To solve the proposed crack problem, the Fourier integral transform method is employed together with Laplace transform, leading to the derivation of a singular integral equation with a generalized Cauchy kernel. It is a simple and convenient method for solving this problem. In the numerical results, the values of mixed-mode stress intensity factors (SIFs) are provided as a function of crack orientation angle. The effects come from the crack orientation and the nonhomogeneous material parameter on the dynamic stress intensity factors (DSIFs) are discussed graphically.

2. Formulation of the problem

As shown in Fig.1, consider the plane problem of an arbitrarily oriented crack located in a functionally graded material. Two rectangular Cartesian coordinate systems, (x, y, z) and (x_1, y_1, z_1), are defined to describe the direction of the material gradient and crack orientation, respectively. The system (x_1, y_1, z_1) is obtained by rotating counterclockwise to the system (x, y, z) with angle θ .The crack is assumed to occupy the region $a \le x_1 \le b$, $y_1 = 0$, $|z_1| < \infty$. The shear modulus μ and mass density ρ in (x_1, y_1, z_1) and (x, y, z) coordinate can be written, respectively, as follows [12]

$$\mu(x_1, y_1) = \mu_0 \exp(\beta_1 x_1 + \beta_2 y_1), \quad \rho(x_1, y_1) = \rho_0 \exp(\beta_1 x_1 + \beta_2 y_1), \tag{1}$$

$$\mu(y) = \mu_0 \exp(\beta y), \quad \rho(y) = \rho_0 \exp(\beta y), \tag{2}$$

where β, μ_0 and ρ_0 are material constants, and $\beta_1 = \beta \sin(\theta), \beta_2 = \beta \cos(\theta)$.

The mixed boundary value problem shown in Fig.1 will be solved under the following conditions

$$\sigma_{y_1 y_1}(x_1, 0^+, t) = \sigma_{y_1 y_1}(x_1, 0^-, t), \quad \sigma_{x_1 y_1}(x_1, 0^+, t) = \sigma_{x_1 y_1}(x_1, 0^-, t), \quad -\infty < x_1 < \infty, \tag{3}$$

$$u(x_1, 0^+, t) = u(x_1, 0^-, t), \quad v(x_1, 0^+, t) = v(x_1, 0^-, t), \quad x_1 < a, \quad \text{or} \quad x_1 > b, \tag{4}$$

$$\sigma_{y_1 y_1}(x_1, 0^+, t) = \sigma_1 H(t), \quad a < x_1 < b, \tag{5}$$

$$\sigma_{x_1 y_1}(x_1, 0^+, t) = \sigma_2 H(t), \quad a < x_1 < b, \tag{6}$$

where $\sigma_1 H(t)$ and $\sigma_2 H(t)$ are the negative of dynamic normal stress and shear stress at the crack plane under external loading in an uncracked specimen. $H(t)$ is the Heaviside function of time t. When $t < 0$, $H(t) = 0$, and when $t \ge 0$, $H(t) = 1$.

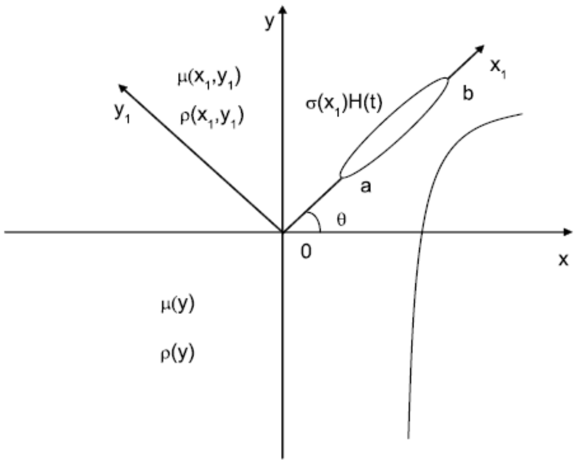

Figure 1. Geometry of the functionally graded material with an arbitrarily oriented crack

3. Method of solutions

The general expressions for displacements components can be written as

$$\hat{u}(x_1, y_1^+, p) = \frac{1}{2\pi}\int_{-\infty}^{\infty}\left[G_1(\xi, p)C_1(\xi, p)e^{\lambda_1(\xi,p)y_1} + G_2(\xi, p)C_2(\xi, p)e^{\lambda_2(\xi,p)y_1}\right]e^{i\xi x_1}\mathrm{d}\xi,$$
$$\hat{v}(x_1, y_1^+, p) = \frac{1}{2\pi}\int_{-\infty}^{\infty}\left[C_1(\xi, p)e^{\lambda_1(\xi,p)y_1} + C_2(\xi, p)e^{\lambda_2(\xi,p)y_1}\right]e^{i\xi x_1}\mathrm{d}\xi, \tag{7}$$

$$\hat{u}(x_1, y_1^-, p) = \frac{1}{2\pi}\int_{-\infty}^{\infty}\left[G_3(\xi, p)C_3(\xi, p)e^{\lambda_3(\xi,p)y_1} + G_4(\xi, p)C_4(\xi, p)e^{\lambda_4(\xi,p)y_1}\right]e^{i\xi x_1}\mathrm{d}\xi,$$
$$\hat{v}(x_1, y_1^-, p) = \frac{1}{2\pi}\int_{-\infty}^{\infty}\left[C_3(\xi, p)e^{\lambda_3(\xi,p)y_1} + C_4(\xi, p)e^{\lambda_4(\xi,p)y_1}\right]e^{i\xi x_1}\mathrm{d}\xi, \tag{8}$$

where $C_j(\xi, p)(j = 1-4)$ are unknown functions, and $\lambda_j(\xi, p)(j = 1-4)$ are the roots of the characteristic equation

$$\lambda^4 + \Omega_1\lambda^3 + \Omega_2\lambda^2 + \Omega_3\lambda + \Omega_4 = 0, \tag{9}$$

where

$$\Omega_1 = 2\beta_2, \quad \Omega_2 = -2\xi^2 + 2i\xi\beta_1 + \beta_2^2 + \frac{(\kappa-3)\beta_1^2}{1+\kappa} - 2\frac{\kappa\rho_0 p^2}{(1+\kappa)\mu_0}, \tag{10}$$

$$\Omega_3 = -2\xi^2\beta_2 + \frac{8i\beta_2\beta_1\xi}{1+\kappa} - 2\frac{\beta_2\kappa\rho_0 p^2}{\mu_0(1+\kappa)}, \tag{11}$$

$$\Omega_4 = \xi^4 - 2i\xi^3\beta_1 - \xi^2\beta_1^2 + \frac{(3-\kappa)\beta_2^2\xi^2}{1+\kappa} + 2\frac{\kappa\rho_0 p^2\xi^2}{\mu_0(1+\kappa)} - \frac{2i\beta_1\rho_0 p^2\kappa\xi}{\mu_0(1+\kappa)} + \frac{-\rho_0^2 p^4 + \rho_0^2 p^4\kappa}{(1+\kappa)\mu_0^2}. \tag{12}$$

Here, $G_j(\xi, p)(j = 1-4)$ can be expressed as

$$G_j(\xi, p) = -\frac{[2i\xi + \beta_1(3-\kappa)]\lambda_j + i\xi\beta_2(\kappa-1)}{(\kappa-1)\lambda_j^2 + \beta_2(\kappa-1)\lambda_j + (i\xi\beta_1 - \xi^2)(\kappa+1) - \rho_0(\kappa-1)p^2/\mu_0}. \tag{13}$$

4. Singular integral equation

Now, we define the following new unknown functions

$$\hat{g}_1(x_1, p) = \frac{\partial}{\partial x_1}[\hat{u}(x_1, 0^+, p) - \hat{u}(x_1, 0^-, p)], \quad a < x_1 < b,$$
$$\hat{g}_2(x_1, p) = \frac{\partial}{\partial x_1}[\hat{v}(x_1, 0^+, p) - \hat{v}(x_1, 0^-, p)], \quad a < x_1 < b. \tag{14}$$

From (3-6), we obtain

$$\int_a^b \frac{\hat{g}_2(t, p)}{t - x_1}\mathrm{d}t + \int_a^b K_{11}(x_1, t, p)\hat{g}_1(t, p)\,\mathrm{d}t + \int_a^b K_{12}(x_1, t, p)\hat{g}_2(t, p)\,\mathrm{d}t = \frac{(\kappa+1)\sigma_1}{2\mu_0 p e^{\beta_1 x_1}},$$
$$\int_a^b \frac{\hat{g}_1(t, p)}{t - x_1}\mathrm{d}t + \int_a^b K_{21}(x_1, t, p)\hat{g}_1(t, p)\,\mathrm{d}t + \int_a^b K_{22}(x_1, t, p)\hat{g}_2(t, p)\,\mathrm{d}t = \frac{(\kappa+1)\sigma_2}{2\mu_0 p e^{\beta_1 x_1}}, \tag{15}$$

where

$$K_{11}(x_1, t, p) = \frac{\kappa+1}{4(\kappa-1)}\Big\{\int_0^A (k_{11} + k_{11c})\cos[\xi(t - x_1)]d\xi + \int_A^\infty (k_{11} + k_{11c} - \frac{2(\kappa-1)\beta_2}{\xi(1+\kappa)})\cos[\xi(t - x_1)]d\xi$$
$$+\int_A^\infty \frac{2(\kappa-1)\beta_2}{\xi(1+\kappa)}\cos[\xi(t - x_1)]d\xi - \int_0^\infty (k_{11} - k_{11c})i\sin[\xi(t - x_1)]d\xi\Big\}, \tag{16}$$

$$K_{12}(x_1,t,p)=\frac{\kappa+1}{4(\kappa-1)}\Big\{\int_0^A(k_{12}+k_{12c})\cos[\xi(t-x_1)]d\xi+\int_A^\infty(k_{12}+k_{12c}-\frac{2(\kappa-1)\beta_1}{\xi(1+\kappa)})\cos[\xi(t-x_1)]d\xi$$
$$+\int_A^\infty\frac{2(\kappa-1)\beta_1}{\xi(1+\kappa)}\cos[\xi(t-x_1)]d\xi-\int_0^\infty(k_{12}-k_{12c}-\frac{4i(\kappa-1)}{\kappa+1})i\sin[\xi(t-x_1)]d\xi\Big\},\tag{17}$$

$$K_{21}(x_1,t,p)=\frac{\kappa+1}{4}\Big\{\int_0^A(k_{21}+k_{21c})\cos[\xi(t-x_1)]d\xi+\int_A^\infty(k_{21}+k_{21c}-\frac{2\beta_1}{\xi(1+\kappa)})\cos[\xi(t-x_1)]d\xi$$
$$+\int_A^\infty\frac{2\beta_1}{\xi(1+\kappa)}\cos[\xi(t-x_1)]d\xi-\int_0^\infty(k_{21}-k_{21c}-\frac{4i)}{\kappa+1})i\sin[\xi(t-x_1)]d\xi\Big\},\tag{18}$$

$$K_{22}(x_1,t,p)=\frac{\kappa+1}{4}\Big\{\int_0^A(k_{22}+k_{22c})\cos[\xi(t-x_1)]d\xi+\int_A^\infty(k_{22}+k_{22c}+\frac{2\beta_2}{\xi(1+\kappa)})\cos[\xi(t-x_1)]d\xi$$
$$-\int_A^\infty\frac{2\beta_2}{\xi(1+\kappa)}\cos[\xi(t-x_1)]d\xi-\int_0^\infty(k_{22}-k_{22c})i\sin[\xi(t-x_1)]d\xi\Big\},\tag{19}$$

$$k_{11}=\frac{i}{\xi}\frac{E_1J_4-E_2J_3}{J_3J_2-J_1J_4},\quad k_{12}=\frac{i}{\xi}\frac{E_2J_1-E_1J_2}{J_3J_2-J_1J_4},\tag{20}$$

$$k_{21}=\frac{i}{\xi}\frac{F_1J_4-F_2J_3}{J_3J_2-J_1J_4},\quad k_{22}=\frac{i}{\xi}\frac{F_2J_1-F_1J_2}{J_3J_2-J_1J_4},\tag{21}$$

$$J_1=G_1+\frac{G_3\left(E_4F_1-E_1F_4\right)}{E_3F_4-F_3E_4}-\frac{G_4\left(E_3F_1-F_3E_1\right)}{E_3F_4-F_3E_4},\tag{22}$$

$$J_2=G_2-\frac{G_4\left(E_3F_2-F_3E_2\right)}{E_3F_4-F_3E_4}+\frac{G_3\left(E_4F_2-E_2F_4\right)}{E_3F_4-F_3E_4},\tag{23}$$

$$J_3=1+\frac{E_4F_1-E_1F_4}{E_3F_4-F_3E_4}-\frac{E_3F_1-F_3E_1}{E_3F_4-F_3E_4},\tag{24}$$

$$J_4=1+\frac{E_4F_2-E_2F_4}{E_3F_4-F_3E_4}-\frac{E_3F_2-F_3E_2}{E_3F_4-F_3E_4}.\tag{25}$$

and $k_{ijc}(i,j=1,2)$ are the complex conjugates of k_{ij}.

The solutions of the singular integral equations Eq.(15) are [14]

$$\hat{g}_1(u,p)=G_1(u,p)/\sqrt{1-u^2},\quad \hat{g}_2(u,p)=G_2(u,p)/\sqrt{1-u^2}.\tag{26}$$

The stress intensity factors in Laplace domain can be defined as

$$\hat{K}_I(a,p)=\lim_{x_1\to a}\sqrt{2(a-x_1)}\sigma_{y_1y_1}(x_1,0)=\frac{2\mu_0e^{\beta_1a}}{\kappa+1}\sqrt{(b-a)/2}G_2(-1,p),\tag{27}$$

$$\hat{K}_I(b,p)=\lim_{x_1\to b}\sqrt{2(x_1-b)}\sigma_{y_1y_1}(x_1,0)=-\frac{2\mu_0e^{\beta_1b}}{\kappa+1}\sqrt{(b-a)/2}G_2(1,p),\tag{28}$$

$$\hat{K}_{II}(a,p)=\lim_{x_1\to a}\sqrt{2(a-x_1)}\sigma_{x_1y_1}(x_1,0)=\frac{2\mu_0e^{\beta_1a}}{\kappa+1}\sqrt{(b-a)/2}G_1(-1,p),\tag{29}$$

$$\hat{K}_{II}(b,p)=\lim_{x_1\to b}\sqrt{2(x_1-b)}\sigma_{x_1y_1}(x_1,0)=-\frac{2\mu_0e^{\beta_1b}}{\kappa+1}\sqrt{(b-a)/2}G_1(1,p).\tag{30}$$

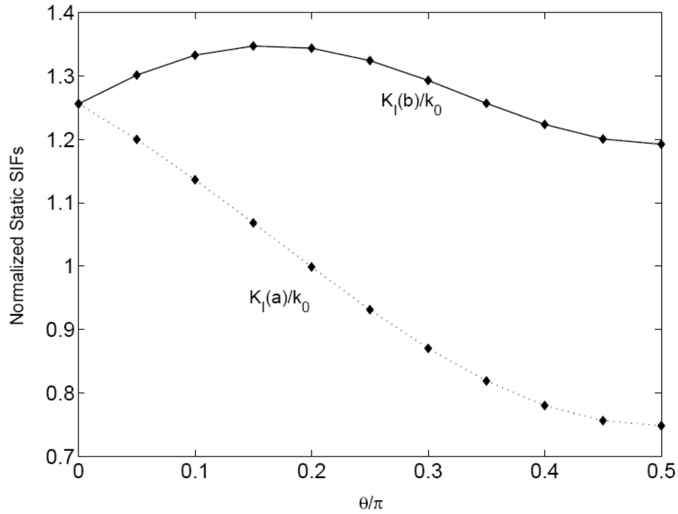

Figure 2. The variation of static SIFs with crack orientation angle θ under crack surface pressure ($\beta a_0 = 1.0$)

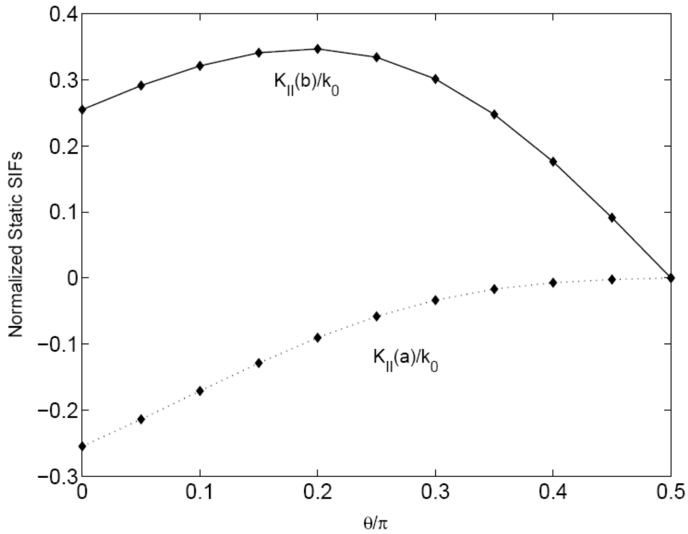

Figure 3. The variation of static SIFs with crack orientation angle θ under crack surface pressure ($\beta a_0 = 1.0$)

The stress intensity factor in the time domain can be obtained from Eqs.(27-30) by using Laplace numerical inversion by Miller and Guy [15].

5. Numerical results and discussion

The following analysis will be conducted under the plane strain state. The surface of the crack loaded by $\sigma_{10}H(t)$ and $\sigma_{20}H(t)$ respectively, where σ_{10} and σ_{20} are constant tractions. Poisson's ratio is taken as $\nu = 0.3$. The dynamic stress intensity factors are normalized by $k_0 = \sigma_{10}\sqrt{a_0}$ and $k = \sigma_{20}\sqrt{a_0}$ for different loads respectively, where $a_0 = (b-a)/2$. $c_2 = \sqrt{\mu_0 / \rho_0}$ is the shear wave velocity, $c_2 t / a_0$ is the non-dimensional time.

Before the analysis, the validity of the analytical solution must be verified. First, we restrict our attention to the crack problem in FGM under static loading. The corresponding static problem was

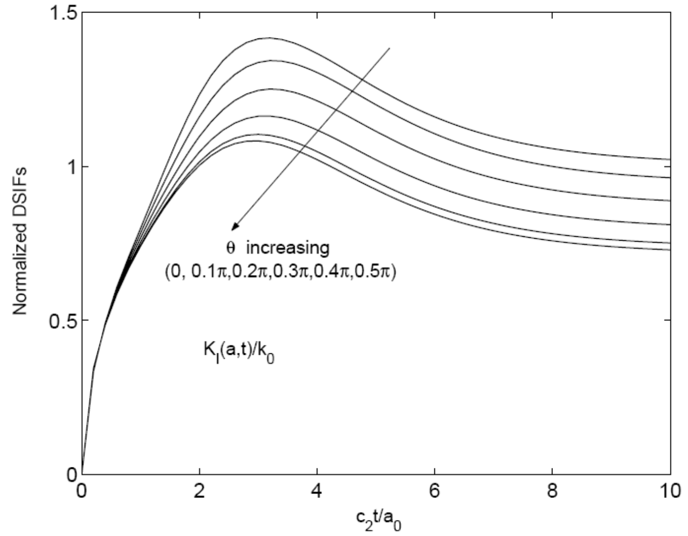

Figure 4. The variation of DSIFs with crack orientation angle θ under crack surface pressure ($\beta a_0 = 0.5$)

studied in [12]. Figs. 2-3 show the variations of the normalized SIFs with the angle θ under the uniform normal traction. These results are very similar to Konda's results [12].

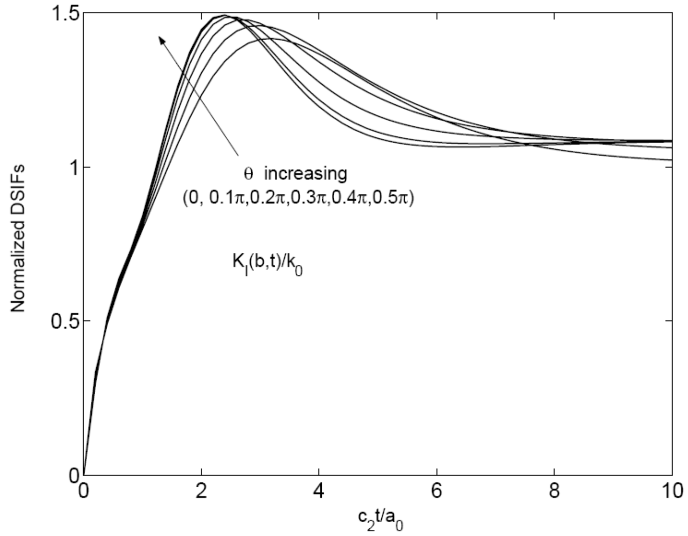

Figure 5. The variation of DSIFs with crack orientation angle θ under crack surface pressure ($\beta a_0 = 0.5$)

Figs.4-5 show the influence of θ on the DSIFs. It can be found that the peak value of $K_I(a,t)/k_0$ decreases with an increase of θ regardless of the value of βa_0. For $\beta a_0 = 0.5$, the peak value of $K_I(b,t)/k_0$ increases with the increasing of θ. And meanwhile, the emergence of time for the DSIFs gradually delays with the decreasing of θ.

Figs.6-7 depict the variations of the normalized mode II DSIFs with the crack direction angle under uniform shear stress when $\beta a_0 = 0.5$. It can be found that the normalized DSIFs increases quickly with time up to the peak, and then the oscillations gradually decay until corresponding steady-state value. The peak time of DSIFs appears more or less for $c_2 t / a_{01} = 1.5$, and then exhibit a slight oscillation after reaching a peak. The peak values of $K_{II}(a,t)/k_0$ and $K_{II}(b,t)/k_0$ increase or decrease with an decrease of θ regardless of the value of βa_0.

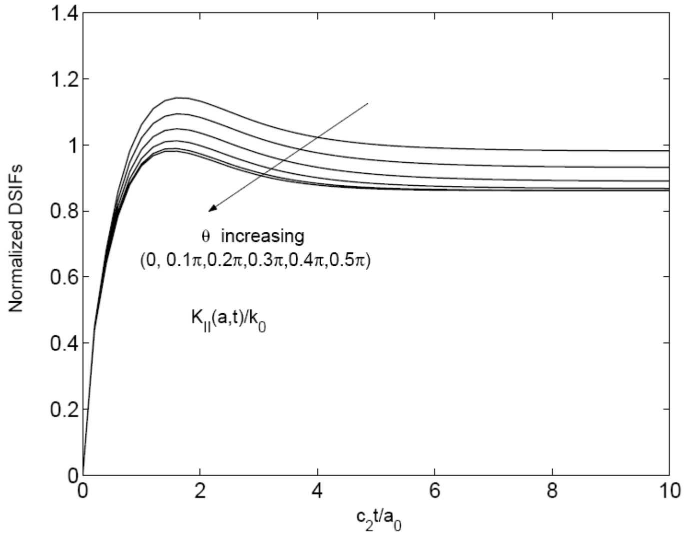

Figure 6. The influence of crack orientation angle θ on the DSIFs under crack surface shear ($\beta a_0 = 0.5$)

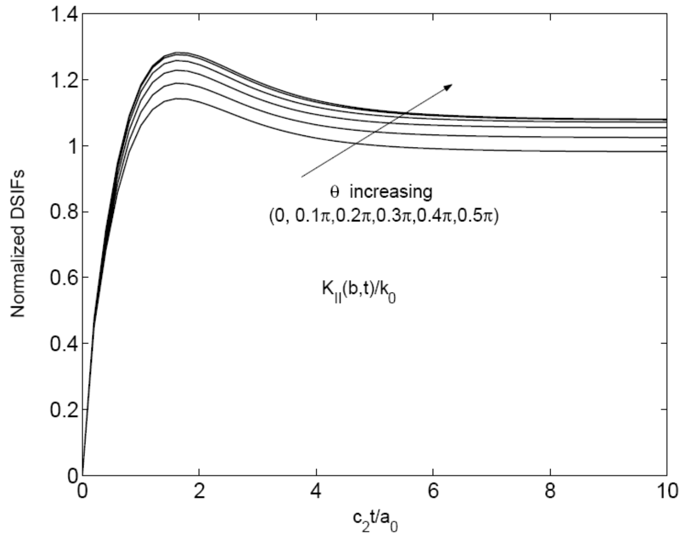

Figure 7. The influence of crack orientation angle θ on the DSIFs under crack surface shear ($\beta a_0 = 0.5$)

Based on the premise that the peak dynamic stress intensity factors may induce brittle fracture, such peaks are plotted in the sequel as a function of the crack orientation angle θ in Figs. 8-9. For $\beta a_0 = 0.5$, as shown in Fig.8, the peak value of the mode I DSIFs in crack tip a increases with an decrease of θ, while the peak value of the mode I DSIFs in crack tip b increases with an increase of θ. For $\beta a_0 = 1.0$ or 1.5, the peak value of the mode I DSIFs in crack tip b increases with θ, going through the maxima at some angle, and then begin to decrease at the enlarged crack obliquity, e.g., $\theta = 0.1\pi$ or 0.15π. The peak value of the mode I DSIFs in crack tip a decreases with an increase of θ. Of interest in the figure is that for the crack angle more than 0.4π, the variation of θ appears to hardly affect the peak stress intensification at the crack tips. From Fig.9, it can be seen that the peak values of crack tips a and b decrease or increase with an increase of θ.

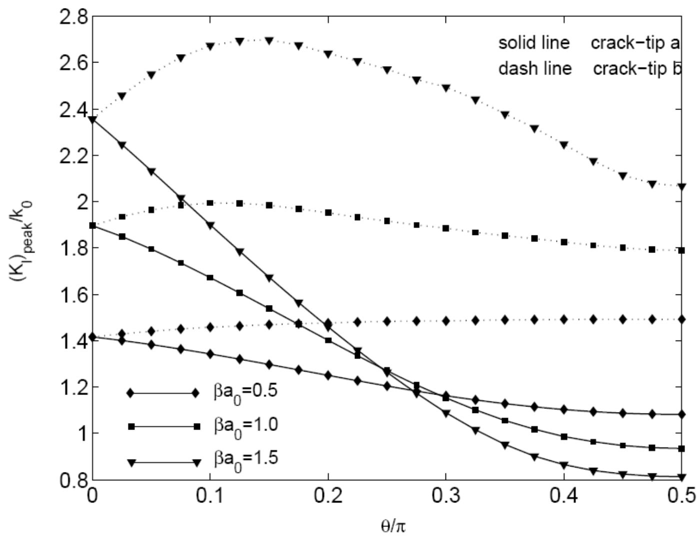

Figure 8. The influence of crack orientation angle θ on the peak values of the DSIFs under crack surface pressure

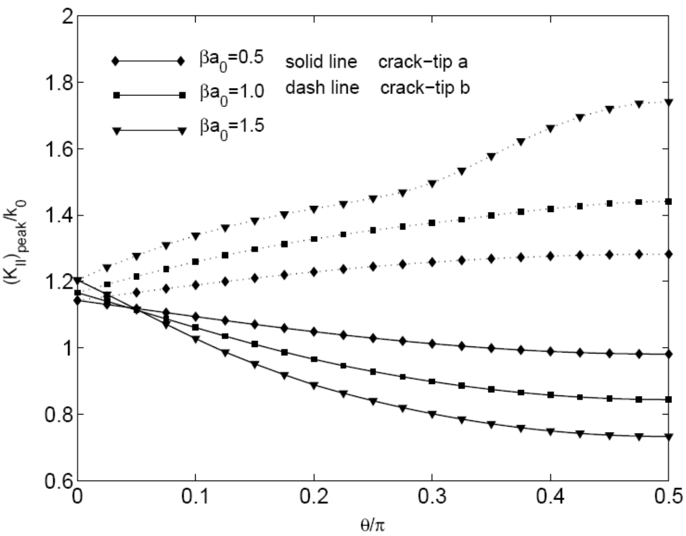

Figure 9. The influence of crack orientation angle θ on the peak values of the DSIFs under crack surface shear

6. Conclusion

The elastodynamic response of an arbitrarily oriented crack in functionally graded materials has been investigated with the aid of the basic plane elasticity equations. The mixed-mode DSIFs evaluated for an arbitrarily oriented crack were shown to be strongly affected by the geometric and loading configuration of the media in conjunction with the material gradations in the nonhomogeneous constituent. The integral transform techniques were employed in conjunction with the coordinate transformations of relevant field variables and a resulting Cauchy-type singular integral equation was solved in the Laplace transform domain. Following the inversion of the Laplace transforms, the evolution of the dynamic mixed-mode DSIFs stress intensity factors with time was evaluated.

Acknowledgements

This work is supported by the National Natural Science Foundation of China (51061015,11261045) and research fund for the doctoral program of higher education of China (20116401110002).

References

[1] Delale, F., Erdogan, F., On the mechanical modeling of the interfacial region in bonded half-planes. J. Appl. Mech., 55(1988) 317-324.
[2] Chen, Y.F., Erdogan, F., The interface crack problem for a nonhomogeneous coating bonded to a homogeneous substrate. J. Mech. Phys. Solids, 44(1996) 771-787.
[3] Huang, G.Y., Wang, Y.S., Yu, S.W., Fracture analysis of a functionally graded interfacial zone under plane deformation. Int.J. Solids Struct., 41(2004) 731-743.
[4] Ding, S.H., Li, X., Anti-plane problem of periodic interface cracks in a functionally graded coating-substrate structure. Int. J.Fract., 153(2008) 53-62.
[5] Ding, S.H., Li, X., Thermal stress intensity factors for an interface crack in a functionally graded layered structures. Archive of Applied Mechanics., 7(2011) 943-955.
[6] Atkinson, C., Some results on crack propagation in media with spatially varying elastic properties. Int. J. Fract. ,11(1975)619-628.
[7] Li, C.Y., Weng, G.J., Dynamic stress intensity factor of a cylindrical interface crack with a functionally graded interlayer. Mech. Mater., 33(2001) 325-333.
[8] Guo, L.C., Wu, L.Z., Ma, L., Zeng, T., Fracture analysis of a functionally graded coating-substrate structure with a crack perpendicular to the interface - Part II: Transient problem. Int. J.Fract., 127(2004)39-59.
[9] Li, Y.D., Lee,K.Y., Yao D., Dynamic stress intensity factors of two collinear mode-III cracks perpendicular to and on the two sides of a bi-FGM weak-discontinuous interface. Eur. J. Mech. A-Solids, 27(2008)808-823.
[10] Ding, S.H., Li, X., Zhou Y.T., Dynamic Stress Intensity Factors of Mode I Crack Problem for Functionally Graded Layered Structures.CMES: Computer Modeling in Engineering & Sciences., 56(2010)43-84.
[11] Bogy, D.B., On the plane elastostatic problem of a loaded crack terminating at a material interface. ASME. J. Appl. Mech., 38 (1971) 911-918
[12] Konda, N., Erdogan, F., The mixed-mode crack problem in nonhomogeneous elastic plane. Eng. Fract. Mech., 47(1994)533-545.
[13] Choi, H.J., Impact behavior of an inclined edge crack in a layered medium with a graded nonhomogeneous interfacial zone: antiplane deformation. Acta Mech., 193(2007)67-84.
[14] Muskelishvili, I. N., Singular integral equations, Groningen: Noordhoff, The Netherlands,1953.
[15] Miller, M. K., Guy, W. T., Numerical inversion of the Laplace transform by the use of Jacobi polynomials. SIAM J. Numer. Anal., 3(1966)624-635.